FUDMA Journal of Sciences (FJS)
ISSN online: 2616-1370
ISSN print: 2645 - 2944
Vol. 5 No. 1, March, 2021, pp 261 – 270
DOI: https://doi.org/10.33003/fjs-2021-0501-564

RO-VIBRATIONAL PARTITION FUNCTION AND MEAN THERMAL ENERGY OF THE IMPROVED WEI OSCILLATOR

[1]Bitrus, B. M., [2]Nwabueze, C. M., [3]Ojar, J. U., [4]Eyube, E. S.

[1, 2]Department of Physics, Faculty of Science, Taraba State University, P.M.B. 1176, Jalingo Taraba State, Nigeria
[3]Department of Basic Science, Adamawa State College of Agriculture, P.M.B. 2088, Ganye, Adamawa State, Nigeria
[4]Department of Physics, School of Physical Sciences, Modibbo Adama University of Technology, P.M.B. 2076, Yola, Adamawa State, Nigeria
[1]Corresponding author's email: bitrusbako10@yahoo.com Tel: 08036913630

ABSTRACT

In this paper, the improved Wei oscillator has been used to model the experimental Rydberg-Klein-Rees data of the $X^2\,\Sigma_g^+$ state of N_2^+ diatomic ions. Average absolute deviation from the dissociation energy of 0.3211% and mean absolute percentage deviation of 0.6107% were obtained. These results are quite satisfactory since they are within error requirement rate of less than 1% of the Lippincott's criterion. Using an existing equation in the literature for bound state ro-vibrational energy, expressions for ro-vibrational partition function and mean thermal energy were derived for the improved Wei oscillator within the context of classical physics. The formulas obtained for ro-vibrational partition function and mean thermal energy were subsequently applied to the spectroscopic data of N_2^+ ($X^2\,\Sigma_g^+$) diatomic ions. Studies have revealed that the partition function of the system decreases monotonically with decrease in temperature and increases with increase in upper bound vibrational quantum number. On the other hand, the mean thermal energies of the diatomic ions show an initial sharp decrease when the temperature is decreased and afterwards remains fairly stable as the temperature is further lowered. The results obtained in this work may find suitable applications in astrophysics were potential energy functions are required to model experimentally determined potential energy data with high precision. The work may also be useful in many other areas of physics which include: chemical physics, molecular physics, atomic physics and solid-state physics.

Keywords: Partition function, Improved Wei potential, Hellmann-Feynman theorem, Ro-vibrational energies, Schrödinger equation

INTRODUCTION

In the subject area of relativistic and nonrelativistic quantum mechanics, knowledge of analytical wave functions has been of central importance due the relevant information they convey about the quantum mechanical system under probe (Ikot et al., 2020a; Eyube et al., 2021). For example, information such as: thermodynamic functions (Oyewumi et al., 2014; Yahya and Oyewumi, 2016), index of refraction (Khordad and Mirhosseini, 2015), Fisher information (Romera et al., 2005; Wu et al., 2019; Ikot et al., 2020b), expectation values (Ikot et al, 2019; Eyube et al., 2020b) and optical properties (Khordad and Mirhosseini, 2015) of the system are some of the vital information that can be retrieved from knowledge of wave functions.

Obtaining wave functions for the description of a quantum mechanical state is quite a daunting task, it requires solving a second order partial differential equation for a given potential energy function (Eyube et al., 2021). A special class of wave equation which is of fundamental importance in this field of research is the Schrödinger equation, it is reported to be a suitable model in the description of spinless particles (Yahya and Oyewumi, 2016).

Various potential energy functions have been used in the literature to solve the Schrödinger equation. Some of the potential energy models used include amongst others: Pöschl-Teller like potential (Dong and Gonzalez-Cisneros, 2008), Kratzer potential (Edet et al., 2019), Tietz-Hua potential and its modified form (Onate et al., 2021) and improved Tietz potential (Tang et al., 2014), just to mention but a few. Analytical solution methods used to arrive at solutions of wave equations are: Nikiforov-Uvarov method (Eshghi et al., 2018), exact and proper quantization rules (Falaye et al., 2015; Eyube et al., 2020a), supersymmetric quantum approach (Onate et al., 2021) and ansatz solution method (Edet et al., 2019), the list is vast.

An important potential energy function which is of central importance to this work is the improved Wei potential, it is given as (Jia et al., 2012; Eyube et al., 2020a; Onate et al., 2020)

$$V(r) = D_e \left\{ 1 - \frac{(1-H)\,\mathrm{e}^{\alpha r_\mathrm{e}}}{\mathrm{e}^{\alpha r} - H\,\mathrm{e}^{\alpha r_\mathrm{e}}} \right\}^2 , \tag{1}$$

where D_e is the dissociation energy, r_e is the equilibrium bond length and the parameters α and H are respectively given by (Eyube et al., 2020a)

$$\alpha = \pi c\, \omega_\mathrm{e} \left(\frac{8\mu}{D_\mathrm{e}} \right)^{\frac{1}{2}} - \frac{32\pi^4 c^2 \mu^2 r_\mathrm{e}^3 \omega_\mathrm{e} \alpha_\mathrm{e}}{3h^2} - \frac{1}{r_\mathrm{e}} , \tag{2}$$

$$H = 1 - \frac{\alpha}{\pi c\, \omega_\mathrm{e}} \left(\frac{D_\mathrm{e}}{2\mu} \right)^{\frac{1}{2}} , \tag{3}$$

where the spectroscopic parameters ω_e and α_e are the equilibrium harmonic vibrational frequency and rotational-vibrational coupling constant, μ is the reduced mass of the system, c is the speed of light and h is the Planck constant.

Recently, Eyube and collaborators (Eyube et al., 2020a) used the ideas of exact quantization rule to obtain the eigen solutions of the D-dimension Schrödinger equation, results obtained were used to study the spectroscopic data of CO diatomic molecule. In another development, eigen solutions, expectation values and Fisher information were obtained for the Wei potential function via supersymmetric quantum technique (Onate et al., 2020).

The present study aims at obtaining the ro-vibrational partition function and mean thermal energy of the improved Wei oscillator, which to the best of our knowledge have never been reported in the literature. This paper is organized as follows. Section 2 deals with the mathematical formulation of the research work, in this section, expressions for ro-vibrational partition function and mean thermal energy were derived. Section 3 is devoted to results and discussion. A brief conclusion of the work is presented in section 4.

MATHEMATICAL FORMULATION

In this section, useful expressions of thermodynamic relations of the improved Wei oscillator is considered. Firstly, expression for ro-vibrational partition function is derived using an existing equation in the literature for bound state ro-vibrational energies, this will in turn be used to obtain expression for the mean thermal energy for the potential.

Ro-vibrational Partition Function

Precise knowledge of partition function is essential, not only does it shows how system of particles are distributed in a given micro/macro state as in statistical mechanics, but other useful thermodynamic quantities are easily expressed as mathematical relations of the partition function. At a given temperature T, the ro-vibrational partition function is defined as (Eyube et al., 2021)

$$Z(\beta) = \sum_{\nu=0}^{\lambda} e^{-\beta E_{\nu J}} , \tag{4}$$

where $\beta = (\mathrm{k_B}\, T)^{-1}$, $\mathrm{k_B}$ being the Boltzmann constant, T is the temperature and parameter λ is the upper bound vibrational quantum number. $E_{\nu J}$ is the ro-vibrational energy eigenvalue of the improved Wei potentials; it is given in three dimensions as (Eyube et al., 2020a; Onate et al., 2020)

$$E_{\nu J} = D_\mathrm{e} + \frac{J(J+1)\hbar^2 c_0}{2\mu} - \frac{\alpha^2\hbar^2}{2\mu} \left\{ \frac{\dfrac{\mu D_\mathrm{e}}{\alpha^2\hbar^2}\left(\dfrac{1}{H^2}-1\right) + \dfrac{J(J+1)}{2\alpha^2 H^2}\left(c_2\,\mathrm{e}^{-2\alpha r_e} - H\,c_1\,\mathrm{e}^{-\alpha r_e}\right)}{\nu + \dfrac{1}{2} + \sqrt{\dfrac{1}{4} + \dfrac{2\mu D_\mathrm{e}}{\alpha^2\hbar^2}\left(\dfrac{1}{H}-1\right)^2 + \dfrac{J(J+1)c_2\,\mathrm{e}^{-2\alpha r_e}}{2\alpha^2 H^2}}} - \frac{\nu + \dfrac{1}{2} + \sqrt{\dfrac{1}{4} + \dfrac{2\mu D_\mathrm{e}}{\alpha^2\hbar^2}\left(\dfrac{1}{H}-1\right)^2 + \dfrac{J(J+1)c_2\,\mathrm{e}^{-2\alpha r_e}}{2\alpha^2 H^2}}}{2} \right\}^2 , \tag{5}$$

where v and J are respectively the vibrational and rotational quantum numbers. The constant coefficients c_0, c_1 and c_2 are defined as (Eyube et al., 2020a)

$$c_0 = \frac{1}{r_e^2} + \frac{1}{\alpha r_e^3}(1-H)(3+H) - \frac{3}{\alpha^2 r_e^4}(1-H)^2, \tag{6}$$

$$c_1 = \frac{2e^{\alpha r_e}}{\alpha r_e^3}(1-H)^2(2+H) - \frac{6e^{\alpha r_e}}{\alpha^2 r_e^4}(1-H)^3, \tag{7}$$

$$c_2 = -\frac{e^{2\alpha r_e}}{\alpha r_e^3}(1-H)^3(1+H) + \frac{3e^{\alpha r_e}}{\alpha^2 r_e^4}(1-H)^4. \tag{8}$$

For the purpose of this work, equation (5) is expressed in the more compact form as

$$E_{vJ} = -\varepsilon\left(\frac{\rho^2}{4} + \frac{\eta^2}{\rho^2} + \frac{\gamma}{\varepsilon}\right), \tag{9}$$

where

$$\varepsilon = \frac{\alpha^2\hbar^2}{2\mu}, \tag{10}$$

$$\rho = v + \frac{1}{2} + \sqrt{\frac{1}{4} + \frac{2\mu D_e}{\alpha^2\hbar^2}\left(\frac{1}{H}-1\right)^2 + \frac{J(J+1)c_2 e^{-2\alpha r_e}}{2\alpha^2 H^2}}, \tag{11}$$

$$\eta = \frac{\mu D_e}{\alpha^2\hbar^2}\left(\frac{1}{H^2}-1\right) + \frac{J(J+1)}{2\alpha^2 H^2}\left(c_2 e^{-2\alpha r_e} - H c_1 e^{-\alpha r_e}\right), \tag{12}$$

$$\gamma = -D_e - \frac{J(J+1)\hbar^2 c_0}{2\mu} - \eta\varepsilon. \tag{13}$$

Substituting equation (9) into (4) leads to

$$Z(\beta) = \sum_{v=0}^{\lambda} e^{\beta\varepsilon\left(\frac{\rho^2}{4}+\frac{\eta^2}{\rho^2}+\frac{\gamma}{\varepsilon}\right)}. \tag{14}$$

In the classical limit, at high temperatures, T and for large λ and small β, the summation in equation (14) can be replaced with an integral (Eyube et al., 2021), this leads to

$$Z(\beta) = \int_0^{\lambda} e^{\beta\varepsilon\left(\frac{\rho^2}{4}+\frac{\eta^2}{\rho^2}+\frac{\gamma}{\varepsilon}\right)} d\rho. \tag{15}$$

With the help of MAPLE software, the definite integral in equation (15) is evaluated as

$$Z(\beta) = \lambda e^{\beta\varepsilon\rho^2+\beta\gamma}\left\{e^{x^2} - \sqrt{\pi}\, x\,\mathrm{erfi}(x) - \sqrt{\pi}\, x\right\}, \tag{16}$$

where

$$x = \frac{\eta}{\lambda}\sqrt{\beta\,\varepsilon}\,, \tag{17}$$

and erfi (x) is the imaginary error function given by (Eyube et al., 2021)

$$\mathrm{erfi}\left(y\right) = -i\,\mathrm{erf}\left(i\,x\right) = \frac{2}{\sqrt{\pi}}\int_0^x e^{z^2}\,\mathrm{d}\,z\,. \tag{18}$$

Ro-vibrational Mean Thermal Energy

The ro-vibrational mean thermal energy is calculated from the expression (Eyube et al., 2021)

$$U\left(\beta\right) = -\frac{\partial}{\partial\beta}\ln Z\left(\beta\right). \tag{19}$$

Inserting equation (16) into (19) and simplifying, we obtained

$$\mathrm{U}\left(\beta\right) = \frac{\sqrt{\pi}}{2\,\beta}\frac{x + x\,\mathrm{erfi}\left(x\right)}{\mathrm{e}^{x^2} - \sqrt{\pi}\,x\,\mathrm{erfi}\left(x\right) - \sqrt{\pi}\,x} - \gamma - \varepsilon\,\rho^2\,. \tag{20}$$

RESULTS AND DISCUSSION

The data in Table 1 shows spectroscopic parameters of the diatomic ion used in the present study.

Table 1: Model parameters of the diatomic ion used in this work

Diatomic ion	Ionic state	Model parameter				
		$\mu/10^{-23}$ (g) [20]	r_e (Å) [20]	D_e (cm^{-1}) [20]	ω_e (cm^{-1}) [21]	α_e (cm^{-1}) [21]
N_2^+	$X^2\sum_g^+$	1.171	1.116	71365	2207.19	0.02

[20] – Kunc and Gordillo-Vázquez, 1997; [21] – Singh and Rai, 1966

With the help of the data in Table 1, equations (2) and (3) were used to compute α and H as 2.658267 Å^{-1} and 0.00510793 respectively. Where necessary, these values will be used in our subsequent calculations.

In order to confirm the applicability of the improved Wei oscillator to the N_2^+ ($X^2\,\Sigma_g^+$) diatomic ion, equation (1) is required to model the experimental Rydberg-Klein-Rees (RKR) data of this diatomic ion, the RKR data are shown in Table 2. As a first step, equation (1) is used to compute V_{min} and V_{max} corresponding to $r = r_{min}$ and $r = r_{max}$ respectively, V is obtained as the arithmetic mean of V_{min} and V_{max}. In Figure 1 both V_{min} and V_{max} are plotted against r_{min} and r_{max} respectively. Also shown in the plot are the experimental data points of V_{RKR} plotted against r_{min} and also $r_{max.}$

As revealed by the plot, most of the experimental data points coincide with the improved Wei potential curve, therefore, the improved Wei potential is a good model for the N_2^+ ($X^2\,\Sigma_g^+$) ion. A quantitative measure of the goodness-of-fit of a potential energy curve to experimental RKR data points is given by the average absolute deviation from the dissociation energy, it is defined by the equation (Tang et al., 2014)

$$\sigma_{\mathrm{ave}} = \frac{100}{N\,D_e}\sum_{v=0}^{N}\left|V_{\mathrm{RKR}}\left(r\right) - V\left(r\right)\right|, \tag{21}$$

where N is the number of experimental data points. When applied to the data in columns 6 and 8 of Table 2, equation (21) gives σ_{ave} as 0.3211% of D_e. This result is in agreement with Lippincott's error requirement of less than 1% of D_e (Tang et al., 2014). Thus, it can be inferred that the improved Wei oscillator is a suitable potential model for the N_2^+ ($X^2\,\Sigma_g^+$) diatomic ion.

Table 2: Computed improved Wei potential (*V*), pure vibrational state energy eigenvalues ($E_{v\,0}$) and literature data for experimental RKR potential (V_{RKR}) for the N_2^+ ($X^2\,\Sigma_g^+$) diatomic ion

v	r_{min} (Å) [20]	r_{max} (Å) [20]	V_{min} (cm^{-1})	V_{min} (cm^{-1})	V (cm^{-1})	$E_{v\,0}$ (cm^{-1})	V_{RKR} (cm^{-1}) [20]
0	1.071	1.167	1056.0	1225.5	1140.8	1094.0	1099.6
1	1.043	1.207	3097.8	3413.9	3255.8	3256.7	3285.9
2	1.024	1.237	5239.7	5539.8	5389.7	5385.6	5417.7
3	1.010	1.263	7270.0	7621.5	7445.7	7480.6	7536.5
4	0.998	1.287	9349.1	9686.2	9517.7	9541.9	9590.5
5	0.988	1.310	11341.4	11756.4	11548.9	11569.3	11648.2
6	0.979	1.331	13350.9	13699.6	13525.3	13563.0	13651.8
7	0.971	1.352	15320.2	15674.0	15497.1	15522.8	15629.7
8	0.964	1.372	17192.5	17568.5	17380.5	17448.8	17570.4
9	0.958	1.392	18913.3	19464.8	19189.0	19341.0	19474.2
10	0.951	1.411	21062.5	21258.5	21160.5	21199.4	21345.1
11	0.946	1.431	22694.7	23130.2	22912.5	23024.0	23180.9
12	0.940	1.450	24764.6	24886.2	24825.4	24814.8	24981.5
13	0.935	1.469	26585.3	26615.3	26600.3	26571.8	26746.2
14	0.930	1.489	28496.3	28401.4	28448.8	28295.0	28479.7
15	0.926	1.508	30092.1	30062.3	30077.2	29984.4	30164.0
16	0.921	1.527	32173.1	31685.0	31929.1	31639.9	31819.8
17	0.917	1.547	33909.0	33349.6	33629.3	33261.7	33436.1
18	0.913	1.567	35709.8	34967.3	35338.5	34849.7	35012.9
19	0.909	1.587	37577.2	36536.6	37056.9	36403.8	36550.2
20	0.905	1.607	39512.9	38056.4	38784.6	37924.2	38048.0

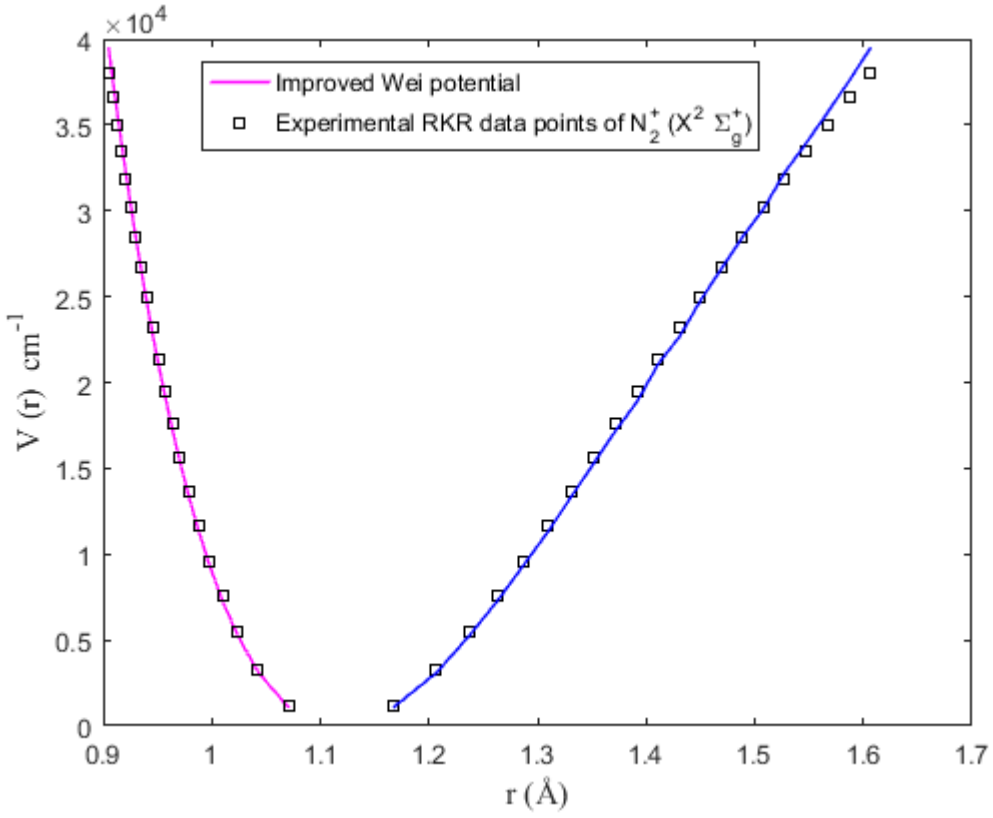

Figure 1: Graphical representation of the improved Wei potential and experimental RKR data as a function of internuclear separation for the N_2^+ ($X^2\,\Sigma_g^+$) diatomic ion

Equation (5) has also been used to compute pure vibrational state bound state energy eigenvalues ($E_{v\,0}$) for the improved Wei oscillator, the calculated energies are shown by the entries in column 7 of Table 2. The $E_{v\,0}$ and experimental RKR energies ($E_{RKR} \approx V_{RKR}$) plotted as a function of rotational quantum number v are shown in Figure 2, the plot clearly shows favorable agreement between $E_{v\,0}$ and E_{RKR}. To quantitatively compare these results, the mean absolute percentage deviation (MAPD) is considered, it is given as (Yanar et al., 2020)

$$\mathrm{MAPD} = \frac{100}{N}\sum_{v=0}^{N}\left|1-\frac{E_{\mathrm{IPTP}}}{E_{\mathrm{RKR}}}\right|, \tag{22}$$

Using equation (22) to the data in columns 7 and 8 gives the MAPD as 0.6107%, this result reveals that bound state energies of N_2^+ ($X^2\,\Sigma_g^+$) diatomic ion computed with equation (5) for the improved Wei oscillator is a near perfect fit for the experimental RKR data of the N_2^+ ($X^2\,\Sigma_g^+$) diatomic ion since the calculated MAPD is less than 1% which is within error requirement.

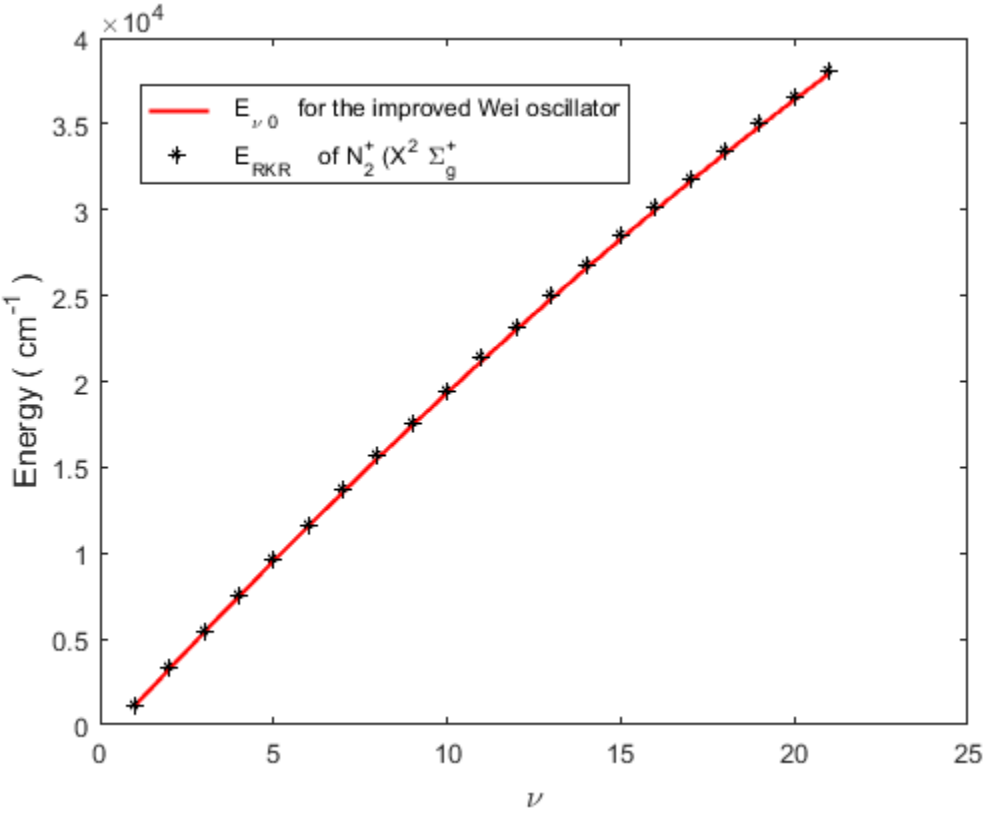

Figure 2: Variation of bound state ro-vibrational energies and experimental RKR energies as a function of vibrational quantum number for the N_2^+ ($X^2\,\Sigma_g^+$) diatomic ion

Having established the relevance of equations (1) and (5) of the improved Wei oscillator in the modeling of experimental RKR data for the N_2^+ ($X^2\,\Sigma_g^+$) diatomic ion. Relations for thermodynamic functions for this potential are now discussed.

With the help of equation (16) and the data in Table 1, Figure 3 shows the graphical representation of the variation of ro-vibrational partition function against parameter β. As it is evident from the plot, it is observed that as the temperature of the system is lowered (or β increased), the ro-vibrational partition function takes a monotonic decrease and is also higher for larger values of upper bound vibrational quantum numbers.

On the other hand, variation of ro-vibrational mean thermal energy versus β is shown by the plot in Figure 4, equation (17) has been used to obtain the plot. The result shows that as β is increased from zero, the system experiences a sharp decrease in internal energy and remain approximately constant as β is further increased. Therefore, it can be deduced that decrease in temperature of the N_2^+ ($X^2\,\Sigma_g^+$) diatomic ions leads to its stability

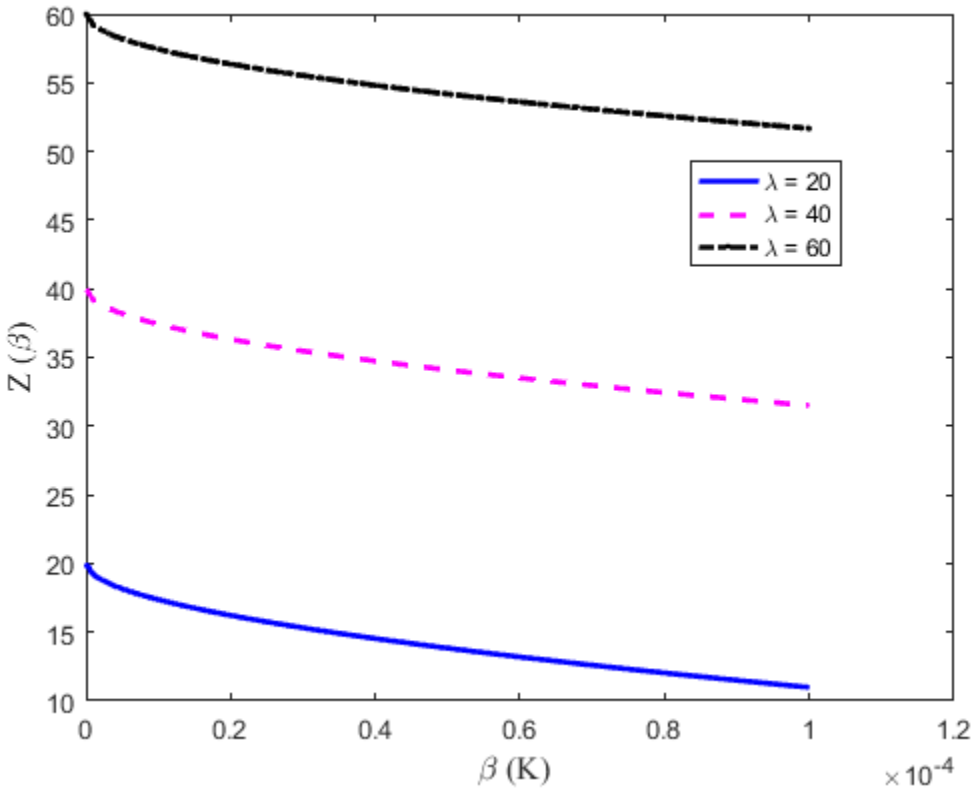

Figure 3: Variation of ro-vibrational partition function as a function of β for different λ

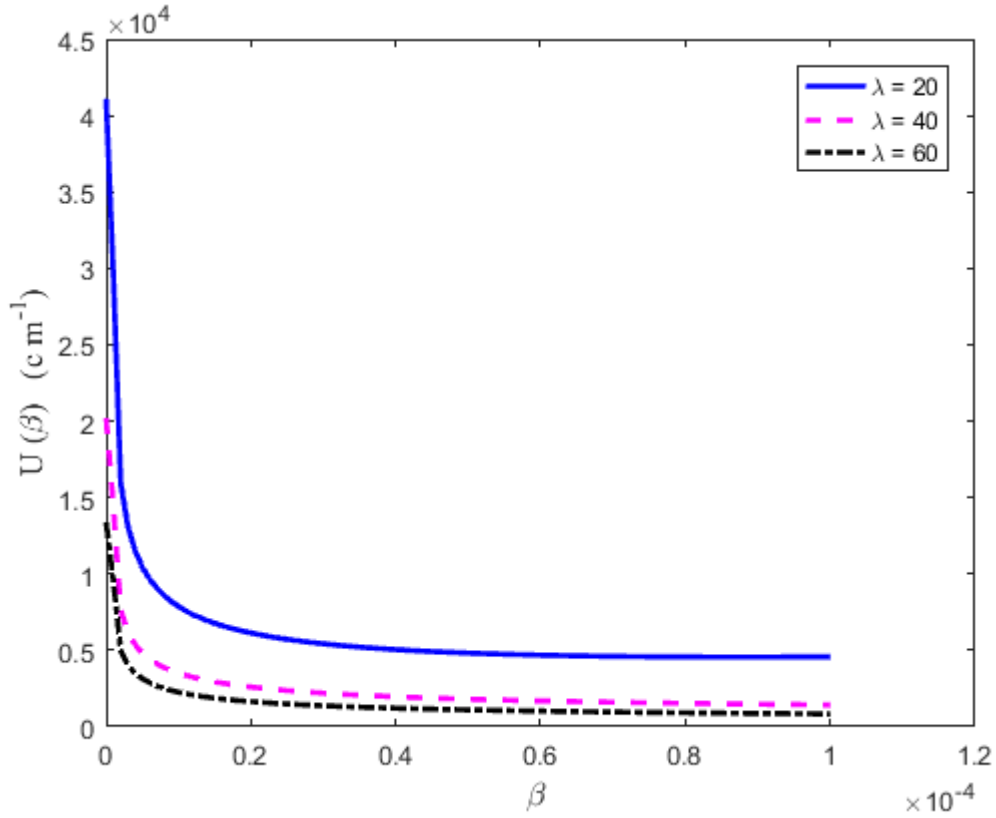

Figure 3: Variation of ro-vibrational mean thermal energy as a function of β for different λ

CONCLUSION

In this work, the improved Wei potential has been employed to model experimentally determined potential energy data for the N_2^+ ($X^2\ \Sigma_g^+$) diatomic ions. Excellent fits (σ_{ave} = 0.3211% of D_e and MAPD = 0.6107%) satisfying the Lippincott's error requirement of less than 1% of dissociation energy were achieved. With the help of the expression for bound state energy eigenvalues of the improved Wei potential, equations for ro-vibrational partition function and mean thermal energy were deduced for the improved Wei potential energy function. The equations obtained were then applied to the spectroscopic parameters of N_2^+ ($X^2\ \Sigma_g^+$) diatomic ions. Our findings show that decrease in temperature of the system amounts to monotonic decrease in partition function of the diatomic ions. Also, it is observed that when the temperature is gradually reduced, the mean thermal energy shows an abrupt decrease after which it remains fairly steady. The results obtained in this study may be useful in many braches of physics such as solid-state physics, chemical physics, atomic physics, astrophysics and molecular physics

REFERENCES

Dong, S.-H. and Gonzalez-Cisneros, A. (2008). Energy spectra of the hyperbolic and second Pöschl–Teller like potentials solved by new exact quantization rule. *Ann. Phys. (N. Y.)* **323**: 1136–1149 https://doi.org/10.1016/j.aop.2007.12.002

Edet, C. O., Okorie, U. S., Ngiangia, A. T. and Ikot, A. N. (2019). Bound state solutions of the Schrodinger equation for the modified Kratzer potential plus screened Coulomb potential. *Indian J. Phys.* **94**: 425-433 https://doi.org/10.1007/s12648-019-01477-9

Eshghi, M., Sever, R. and Ikhdair, S. M. (2018). Energy states of the Hulthén plus Coulomb-like potential with position-dependent mass function in external magnetic fields. *Chin. Phys. B* **27**: 020301 https://doi.org/10.1088/1674-1056/27/2/020301

Eyube, E. S., Yabwa, D. and Wadata, U. (2020a). Rotational-vibrational eigensolutions of the D-dimensional Schrödinger equation for the improved Wei potential. *FJS*, **4**: 269-283 https://doi.org/10.33003/fjs-2020-0402-174

Eyube, E. S., Ahmed, A. D. and Timtere, P. (2020b). Eigensolutions and expectation values of shifted-rotating Möbius squared oscillator. *Eur. Phys. J. Plus* **135**: 893 https://doi.org/10.1140/epjp/s13360-020-00915-6

Eyube, E.S., Yerima, J.B. and Ahmed, A.D. (2021). J – state solutions and thermodynamic properties of the Tietz oscillator. *Phys. Scr.* **96**: 055001 https://doi.org/10.1088/1402-4896/abe3be

Falaye, B. J., Ikhdair, S. M. and Hamzavi, M. (2015). Shifted Tietz–Wei oscillator for simulating the atomic interaction in diatomic molecules. *J. Theor. Appl. Phys.* **9**: 151–158 https://doi.org/10.1007/s40094-015-0173-9

Ikot, A. N., Okorie, U. S., Sever, R. and Rampho, G. J. (2019). Eigensolution, expectation values and thermodynamic properties of the screened Kratzer potential. *Eur. Phys. J. Plus*. **134**: 386 https://doi.org/10.1140/epjp/i2019-12783-x

Ikot, A.N., Okorie, U.S., Osobonye, G. Amadi, P.O., Edet, C.O., Sithole, M.J., Rampho, G.J. and Sever, R. (2020a). Superstatistics of Schrödinger equation with pseudo-harmonic potential in external magnetic and Aharanov-Bohm fields. *Heliyon* **6**: e037738 https://doi.org/10.1016/j.heliyon.2020.e03738

Ikot, A. N., Rampho, G. J., Amadi, P. O., Sithole, M. J., Okorie, U. S., & Lekala, M. I. (2020b). Shannon entropy and Fisher information-theoretic measures for Mobius square potential. The *Eur. Phys. J. Plus*. **135**:503 https://doi.org/10.1140/epjp/s13360-020-00525-2

Jia, C.-S., Diao, Y.-F., Liu, X.-J., Wang, P.-Q., Liu, J.-Y. and Zhang, G.-D. (2012). Equivalence of the Wei potential model and Tietz potential model for diatomic molecules. *J. Chem. Phys*. **137**: 014101 https://doi.org/10.1063/1.4731340

Khordad, R. and Mirhosseini, B. (2015). Application of Tietz potential to study optical properties of spherical quantum dots. *Pramana J. Phys.* **85***:* 723–737 https://doi.org/10.1007/s12043-014-0906-3

Kunc, J. A. and Gordillo-Vázquez, F. J. (1997). Rotational−Vibrational Levels of Diatomic Molecules Represented by the Tietz−Hua Rotating Oscillator. *J. Phys. Chem. A* **101**: 1595–1602 https://doi.org/10.1021/jp962817d

Onate, C.A., Onyeaju, M.C., Bankole, D.T. and Ikot, A.N. (2020). Eigensolution techniques, expectation values and Fisher information of Wei potential function. *J. Mol. Model*. **26**: 311 https://doi.org/10.1007/s00894-020-04573-4

Onate, C.A., Onyeaju, M.C., Omugbe, E., Okon, B.I. and Osafile, O.E. (2021). Bound-state solutions and thermal properties of the modified Tietz-Hua potential. *Scientific Reports*. **11**: 2129 https://doi.org/10.1038/s41598-021-81428-9

Oyewumi, K. J., Falaye, B. J., Onate, C. A., Oluwadare, O. J. and Yahya, W. A. (2013). Thermodynamic properties and the approximate solutions of the Schrödinger equation with the shifted Deng–Fan potential model. *Mol. Phys*. **112**: 127–141 https://doi.org/10.1080/00268976.2013.804960

Romera, E., Sánchez-Moreno, P. and Dehesa, J. S. (2005). The Fisher information of single-particle systems with a central potential. *Chem. Phys. Lett.* **414**: 468–472 https://doi.org/10.1016/j.cplett.2005.08.032

Singh, R. B. and Rai, D. K. (1966). Potential-energy curves for O_2^+, N_2^+ and CO^+. *J. Mol. Spectrosc.* **19**: 424–434 https://doi.org/10.1016/0022-2852(66)90265-7

Tang, H.-M., Liang, G.-C., Zhang, L.-H., Zhao, F. and Jia, C.-S. (2014). Molecular energies of the improved Tietz potential energy model. *Can. J. Chem*. **92**: 201–205 https://doi.org/10.1139/cjc-2013-0466

Wu, L., Zhang, S. and Li, B. (2019). Fisher information for endohedrally confined hydrogen atom. *Phys. Lett. A* **384**: 126033 https://doi.org/10.1016/j.physleta.2019.126033

Yahya, W. A. and Oyewumi, K. J. (2016). Thermodynamic properties and approximate solutions of the ℓ-state Pöschl–Teller-type potential. *J. Assoc. Arab Univ. Basic Appl. Sci*. **21**: 53–58 https://doi.org/10.1016/j.jaubas.2015.04.001

Yanar, H., Taş, A., Salti, M. and Aydogdu, O. (2020). Ro-vibrational energies of CO molecule via improved generalized Pöschl–Teller potential and Pekeris-type approximation. *Eur. Phys. J. Plus*, **135**: 292 https://doi.org/10.1140/epjp/s13360-020-00297-9